

Fortgeschrittenes Physik Lab SS19

Experiment: Spectroscopy at the Iodine Molecule

(Durchgeführt am: 10.10.19 bei Sarcevic, Nikolina)

Erik Bode, Damian Lanzenstiel
(Group 103)

October 25, 2019

Abstract

Contents

| | | |
|----------|--|-----------|
| 1 | Theory | 2 |
| 1.1 | Born-Oppenheimer-Approximation | 2 |
| 1.2 | Franck-Condon-Principle | 2 |
| 1.3 | Morse Potential | 3 |
| 1.4 | Birge-Sponer-Plot | 4 |
| 1.5 | Spectroscopic Notation and Transition Rules | 5 |
| 1.6 | Iodine Tube | 5 |
| 1.7 | CCD-Spectrometer | 6 |
| 1.8 | Monochromator | 6 |
| 2 | Setup and Procedure of the Experiment | 7 |
| 2.1 | Measuring the Absorption Spectrum | 7 |
| 2.2 | Calibration of the Monochromator | 7 |
| 2.3 | Emission Spectrum | 8 |
| 3 | Analysis of the Measurements | 9 |
| 3.1 | Absorption Spectrum | 9 |
| 3.1.1 | Calculating $\omega_e x_e$ and ω_e | 10 |
| 3.1.2 | Dissociation Energy | 11 |
| 3.1.3 | Excitation Energy T_e and Dissociation Energy E_{diss} | 12 |
| 3.1.4 | The Morse Potential | 13 |
| 3.2 | Emission Spectrum | 13 |
| 3.2.1 | Calibration of the Monochromator | 13 |
| 3.2.2 | Laser Peak | 15 |
| 3.2.3 | I_2 Emission Spectrum | 16 |
| 4 | Discussion of the Results | 18 |
| 4.1 | Absorption Spectrum | 18 |
| 5 | Bibliography | 19 |
| | References | 19 |
| 6 | Anhang | 20 |

1 Theory

More detailed information on the theory of the experiment can be found in the 'Staatsexamen' by Martin Meyer.[3]

1.1 Born-Oppenheimer-Approximation

For molecules with two atoms the time-independent Schrödinger equation gives the eigenfunctions and eigenvalues. For these two interacting particles equation 1 defines the Hamilton operator.

$$H = -\frac{\hbar^2}{2m}\nabla + \frac{q_a q_b}{r} \quad (1)$$

As a approximate solution for the time-independent Schrödinger

$$\Psi = \Psi_E \cdot \Psi_N \quad (2)$$

can be used. Ψ_E and Ψ_N are solutions of the separated eq.3 and 4. These describes the movement of the electrons and the movement of the core separately.

$$H_E \Psi_E = (T_E + V_{EE} + V_{EN}) \Psi_E = E_E \Psi_E \quad (3)$$

$$H_N \Psi_N = (T_N + V_{NN} + V_E) \Psi_N = E_N \Psi_N \quad (4)$$

This so called Born-Oppenheimer-Approximation can be used since the electrons move much faster than the cores duo to their huge mass. That also means the electrons can adapt very fast to new distance between the cores and are almost not affected by the movement of the cores.

1.2 Franck-Condon-Principle

The Franck-Condon-Principle works on a similar assumption as the Born-Oppenheimer-Approximation. The idea is that an electronic transitions happen so fast, that they don't affect the slow moving cores, which results in the straight lines from one potential to the other one in figure 1. The principle describes the likelihood of these transition which depend on how much the ground and the excited potential overlay. The Franck-Condon-Factor 5 gives this probability.

$$FC(v_i, v_k) = \left| \int \Psi_{\text{vib}}(v_i) \Psi_{\text{vib}}(v_k) dR \right|^2 \quad (5)$$

Here Ψ_{vib} is the vibration wave function and v_i and v_k are the vibration numbers for the excited and ground state.

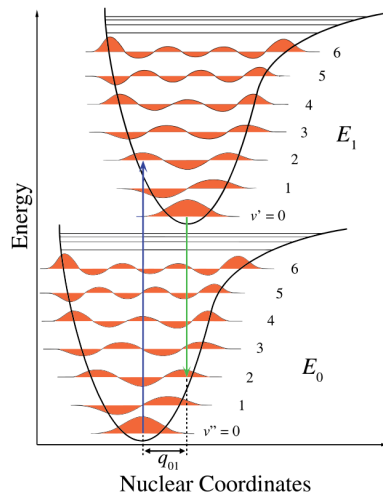


Figure 1: Schematic representation of two atomic states with an example of two atomic molecules. The green and blue line represent the electronic transitions between these states, while the different vibration states $v' = v_i$ and $v'' = v_k$ of the two states are in orange.[6]

1.3 Morse Potential

To describe an oscillation wave function without the rotation only the form of the potential energy is required. Often a harmonic potential is enough but especially for greater distances R between the cores it shows huge differences to the real potential (see figure 2). To describe the potential better for huge values of R the Morse potential can be used. The Morse Potential is an anharmonic one and is defined by equation 6:

$$E_{\text{Pot}}(R) = D_e \times [1 - e^{-a(R-R_e)}]^2 \quad (6)$$

Here D_e is the potential depth or the dissociation energy, a is a molecule constant, R_e is the equilibrium bond distance and R is the distance between the atoms.

The advantage of the Morse potential to a harmonic one is that it describes the real potential good for $R \Rightarrow \infty$ and for $R = R_e$. For $R \ll R_e$ the approximation is as good as a harmonic one. By using this equation to solve the Schrödinger equation, following 'eigenenergy' can be determined:

$$E_{\text{vib}} = \hbar\omega_e \left(v + \frac{1}{2}\right) - \hbar\omega_e x_e \left(v + \frac{1}{2}\right)^2 \quad \text{with} \quad \omega_e x_e = \frac{a^2 \hbar}{4\pi c \mu} \quad \omega_e = a \sqrt{\frac{\hbar D_e}{\pi c \mu}} \quad (7)$$

With that the dissociation energy D_e can be calculated using equation 8:

$$D_e = \frac{\omega_e^2}{4\omega_e x_e} \quad (8)$$

With that the Morse potential gives the easiest extension of the harmonic oscillator by a term of the next higher order in the energy spectrum.

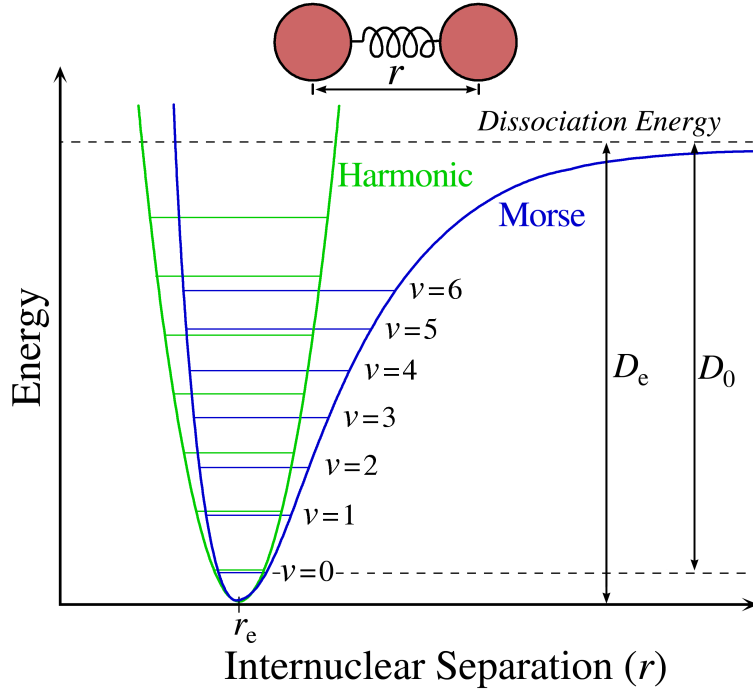


Figure 2: Forms of the Morse in comparison to a Harmonic Potential. The dissociation or bonding energy D_e which is higher than the energy D_0 which is needed to leave the potential.[5]

1.4 Birge-Sponer-Plot

The Birge-Sponer-Plot is a Method to calculate the dissociation energy D_e as well as the values of ω_e and x_e . Here we use the equation 9 as equation of the different energy level by assuming an anharmonic oscillator.

$$G(v) = \frac{E_{\text{vib}}}{hc} = \omega_e(v + \frac{1}{2}) - \omega_e x_e(v + \frac{1}{2})^2 + \omega_e y_e(\frac{1}{2})^3 + \dots \quad (9)$$

The differences between two adjusted energy levels is given by:

$$\Delta G(v + \frac{1}{2}) = G(v + 1) - G(v) = \omega_e - \omega_e x_e(2v + 2) + \omega_e y_e(3v^2 + 6v + \frac{13}{4}) + \dots \quad (10)$$

For an anharmonic potential the differences are getting smaller for higher v . In the potential well the highest state at which the molecule dissociated is called v_{dis} . Above $G(v_{\text{dis}})$ is an energy continuum in which the molecule is dissociated (see fig.3). Plotting $G(v + \frac{1}{2})$ against $v + \frac{1}{2}$ is called the Birge-Sponer-Plot. With it and equation 10 the constants ω_e and $\omega_e x_e$ can be calculated. With them D_e can be calculated using equation 8.

Another way to get D_e is to calculate the energy D_0 with the sum of the different energy distances $G(v + \frac{1}{2})$:

$$D_0 = \sum_{v=0}^{v_{\text{dis}}} \Delta G(v + \frac{1}{2}) \quad (11)$$

The dissociation energy D_e is than:

$$D_e = G(0) + D_0 \quad (12)$$

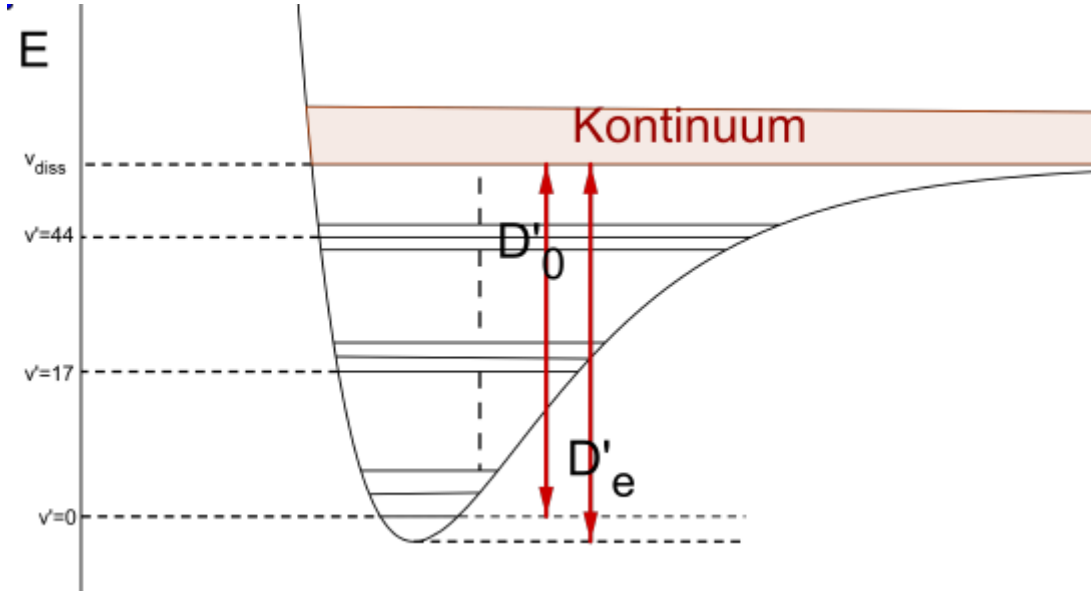


Figure 3: Energy level with continuum and dissociation energy as well as D_0 that is smaller by $G(0)$. [3]

1.5 Spectroscopic Notation and Transition Rules

For the experiment the transition between the I^2 excited state and its ground state is used.

$$X^1\Sigma_{0g}^+ \leftrightarrow B^3\Pi_{0u}^+ \quad (13)$$

The notation of molecule states is normally in the form of:

$$^{2S+1}\Lambda_{\Omega,u/g}^{+/-} \quad (14)$$

- S being the quantum number of the total electron spin.
- Ω is the projection of the total angular momentum $\vec{S} + \vec{L}$ on the molecular axis.
- $+/-$ is the reflection symmetry along an arbitrary plane containing the internuclear axis.
- g/u is for is the effect of the point group operation \hat{i} .
- Λ is the projection of the orbital angular momentum along the internuclear axis

The letter X stands for ground state and letters (A, B, \dots) stands for excited states. For electronic dipole transitions there are the following rules:

- $g \leftrightarrow u, g \leftrightarrow g, g \leftrightarrow g$
- $\Delta\Omega = 0, 1, -1$
- $\Delta\Lambda = 0, 1, -1$
- $\Delta S = 0$

The reason why our transition doesn't contradict these rules is the strong spin-orbit coupling. This acts as a perturbation that mixes states of different multiplicity.

1.6 Iodine Tube

The used iodine Tube is 50 cm long and has a radius of 2 cm and is filled with iodine. The Tube itself is inside a metal sheathing to eliminate stray light. At one side of the tube is a slit which can regulate the intensity of the light leaving the tube. For the experiment iodine is used since it has a broad absorption band system in the visible spectrum as well as the fact that there is only one stable iodine isotope.

1.7 CCD-Spectrometer

A charged coupled device (CCD) is a device that relies on the photo electric effect. It is made of a doped semiconductor. It saves the information of an incoming photons by create a electron, hole pair which can't drain off because of an applied voltage. By opening the potential well the saved electrons can be readout.

The CCD is only a part of the whole device which can be seen in figure 4. It also has two mirrors to direct the incoming light and a lattice to create the spectrum. The CCD is only to read save the information which can be seen using the program **SpectraSuit**. The used spectrometer has a slit width of $5\text{ }\mu\text{m}$ a wavelength range of $400 - 719\text{ nm}$ and a spectral resolution of 0.4 nm .

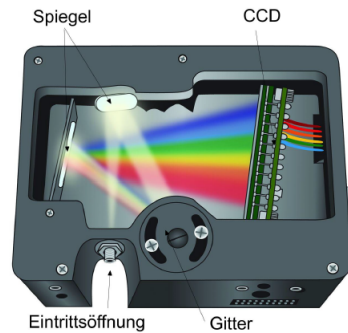


Figure 4: Structure of the CCD Spectrometer. The incoming light gets reflected on the lattice and from there to the CCD where the information is readout.[3]

1.8 Monochromator

The monochromator is used to get measure the spectrum of incoming light. The light gets reflected inside the device to a lattice which splits up the light into a spectrum. The light gets again reflected to the exited where a photometer is fixed. The lattice can be rotated with the help of the engine to pass through the spectrum. The Setup can be seen in figure 5. In the input and exit of the monochromator are two slits to regulate the incoming and exiting light. It is important to note that the slit width should can be set between $5\text{ }\mu\text{m}$ and $2000\text{ }\mu\text{m}$, also the slit width can be set smaller this should never be done. To read the information the program **JodAnalog** is used.

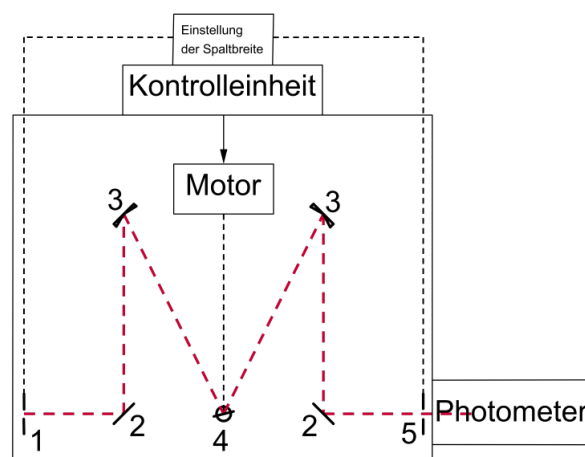


Figure 5: This is a picture of the inside of the monochromator. 1 and 5 are the input and exit slits of the monochromator. With the help of the four mirrors 2 and 3 the light gets directed to exit and the lattice, which is at 4.[3]

2 Setup and Procedure of the Experiment

2.1 Measuring the Absorption Spectrum

First the Absorption Spectrum of I_2 is measured. For this the setup in figure 6 is used.

A Halogen lamp is used as a source of light and parallelised by a lens and refracted into an iodine tube which contains a iodine gas. After this it is focused into an CCD-Spectrometer where the spectrum is measured. To read the spectrum at the computer the program SpectraSuite is used. For the measurement a integration time of 100 ms was chosen. The measurement itself was done six times with only one scan. After this we discovered the ability to take the mean of multiple scans. We chose 30 scans and did another measurement.

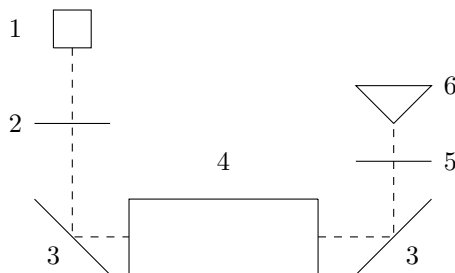


Figure 6: Experimental Setup for measuring the absorption spectrum. 1 Halogen Lamp, 2 paralleling Lens, 3 Mirror, 4 Iodine Tube, 5 focus lens, 6 CCD-Spectrometer.

2.2 Calibration of the Monochromator

Before measuring the emission spectrum with the monochromator it has to be calibrated. For this a mercury vapour lamp is used instead of the halogen lamp. Also the second mirror is switched with the lens so that it know can be focus into the monochromator. In figure 7 the new setup can be seen. Since the x-Axis of the monochromator can't be trusted the start point as well as the end point were noted. As a step width $1 \frac{\text{\AA}}{\text{s}}$ were chosen while the entrance slit was set to $50 \mu\text{m}$. With this the first measurement was done. In the first one it was noticed, that that one of the peaks overshot. That's why we changed the settings at the discriminator level. With that the calibration measurement was done.

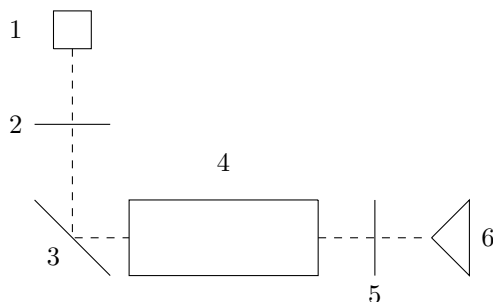


Figure 7: Experimental Setup for calibrating the monochromator via a mercury vapour lamp. 1 Mercury Vapour Lamp, 2 paralleling Lens, 3 Mirror, 4 Iodine Tube, 5 focus Lens, 6 Monochromator.

2.3 Emission Spectrum

For the actually measurement of the Emission Spectrum the setup in figure 8 was used. Here the iodine gas gets excite directly with a laser. First the laser needs to be directed with a mirror into the tube which isn't drawn into the sketch. After the tube the emitted light gets focused with two lenses into the monochromator. Here it is important to note that the red circle that is visible is only a reflection of the lenses and not the real focus point. The real point is not visible but is in the middle of the red circle.

After calibrating the point and heating the tube a bit the resonance laser peak was measured. As start point a wavelength of 6320 \AA and a step width of $1 \frac{\text{\AA}}{\text{s}}$ was chosen. The entrance slit was left at $50 \mu\text{m}$. After this measurement was taken the fluorescence spectrum from 6400 \AA to 8000 \AA . Here the slit with was changed to $360 \mu\text{m}$. Since the measurement needed a while the step with was set to $2 \frac{\text{\AA}}{\text{s}}$ to find a good value for the discriminator. For the later measurements it was set back to $1 \frac{\text{\AA}}{\text{s}}$.

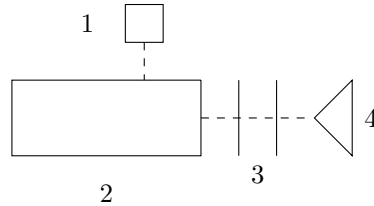


Figure 8: Experimental Setup for measurement of the emission spectrum with the monochromator via a laser. 1 Laser, 2 Iodine Tube, 3 focus Lenses, 4 Monochromator.

3 Analysis of the Measurements

3.1 Absorption Spectrum

First we analyse the measurement of the absorption spectrum with the CCD-Spectrometer. Here only the measurement over 30 scans `abs30.csv` is used. First the whole spectrum was plotted in figure 9. The

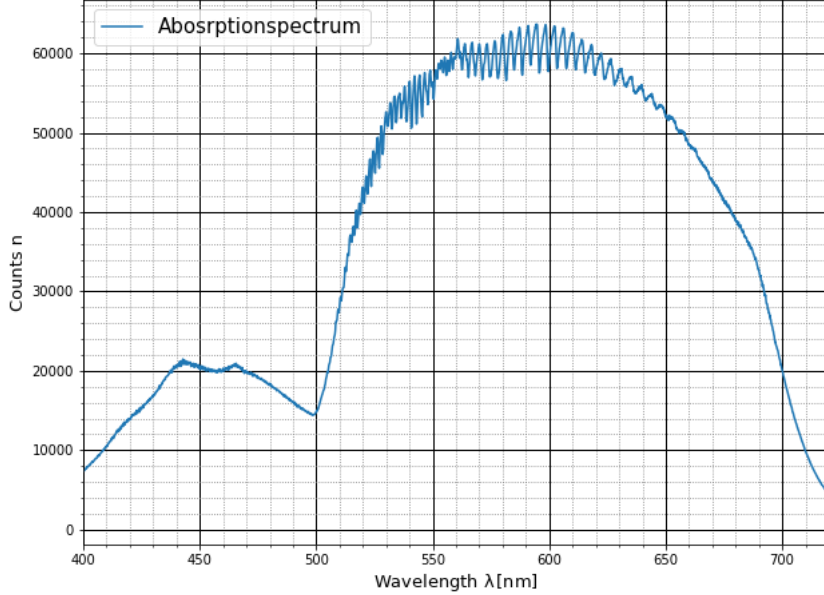


Figure 9: Here is the complete absorption spectrum from 400nm to 720 nm. Measured with the CCD-Spectrometer.

spectrum goes from 400 nm to 720 nm. In the spectrum we are interested in the vibration transitions, which can be seen as dips in the spectrum. In the manual[?] the transition $\nu'' = 0 \rightarrow \nu' = 25$ at a wavelength of 545.8 nm is given as reference. That's why the area of 505 nm to 570 nm was picked to find further transitions, which can be seen in figure 10.

To find the peaks the spectrum was inverted and the Python package `PeakUtils` was used to find the peaks. In figure 10 the furthest to the right marked peak is the reference peak of the $\nu'' = 0 \rightarrow \nu' = 25$ transition. Further to the right are also peaks visible, but they are starting to mix with other peaks which indicates that here another transition superimposes on the first one. That's the reason these peaks were left out. Overall the transitions from $\nu'' = 0 \rightarrow \nu' = 25$ to $\nu'' = 0 \rightarrow \nu' = 47$ were likely found. The positions are noted inside the table 3. Here an error of 0.5 nm was estimated since `PeakUtils`[4] doesn't give errors on the positions.

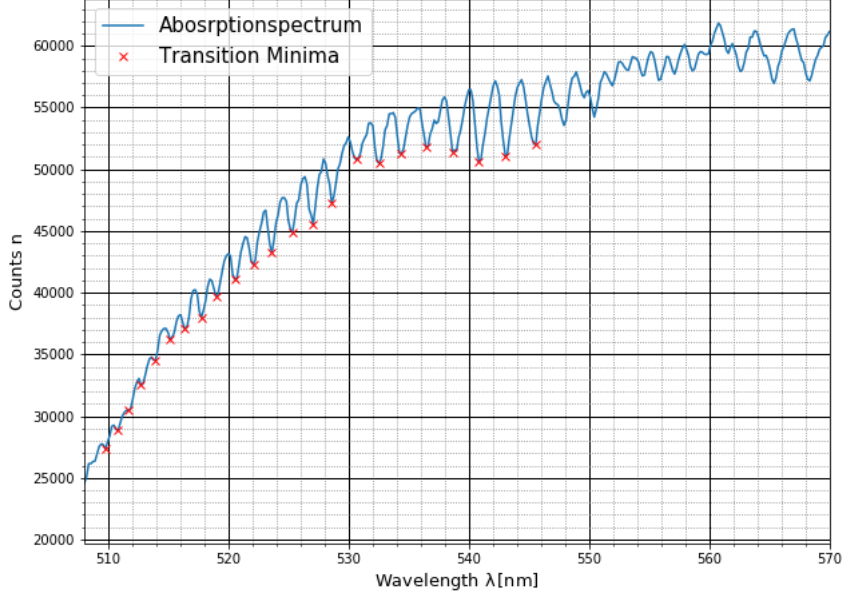


Figure 10: Absorption spectrum from 509 nm to 570 nm. In red are the absorption minima of the different vibration transitions. Starting left with the $\nu'' = 0 \rightarrow \nu' = 47$ transition till at the right side we got the $\nu'' = 0 \rightarrow \nu' = 25$ reference transition.

3.1.1 Calculating $\omega_e x_e$ and ω_e

With these positions a Birge-Sponer-Plot can be created to calculate the constants ω_e and $\omega_e x_e$. For this the wavelength were used to calculate the energy of the absorbed photons. For this Equation 15 was used. The error was like all calculated with the python package `uncertainties`[2] which itself uses Gaussian propagation of uncertainties.

$$G(\nu'') = \frac{1}{\lambda}, \quad \sigma_G = \frac{\sigma_\lambda}{\lambda^2} \quad (15)$$

Since the energy difference between two adjacent transitions $\Delta G(\nu + \frac{1}{2})$ is needed for the plot these were calculated next.

$$\Delta G(\nu + \frac{1}{2}) = G(\nu + 1) - G(\nu) \quad (16)$$

The error is calculated with the following equation:

$$\sigma_{\Delta G} = \sqrt{\sigma_{G(\nu+1)}^2 + \sigma_{G(\nu)}^2} \quad (17)$$

These are now plotted against $\nu + \frac{1}{2}$ in figure 11. By fitting a line of the form $y = mx + b$ to these values the constants can be calculated using equation 18 and 19.

$$\omega_e x_e = -\frac{m}{2}, \quad \sigma_{\omega_e x_e} = -\frac{\sigma_m}{2} \quad (18)$$

$$\omega_e = b + \omega_e x_e, \quad \sigma_{\omega_e} = \sqrt{\sigma_b^2 + \sigma_{\omega_e x_e}^2} \quad (19)$$

The fit was realised using the python package `curve_fit`[1] which also considers the errors in the y direction. With that the following parameters were calculated:

$$m = (-2.09 \pm 0.13) \text{ cm}^{-1} \quad \text{and} \quad b = (133 \pm 4) \text{ cm}^{-1}$$

For the two constants $\omega_e x_e$ and ω_e we get:

$$\begin{aligned} \omega_e &= (135 \pm 5) \text{ cm}^{-1} \\ \omega_e x_e &= (1.04 \pm 0.07) \text{ cm}^{-1} \end{aligned}$$

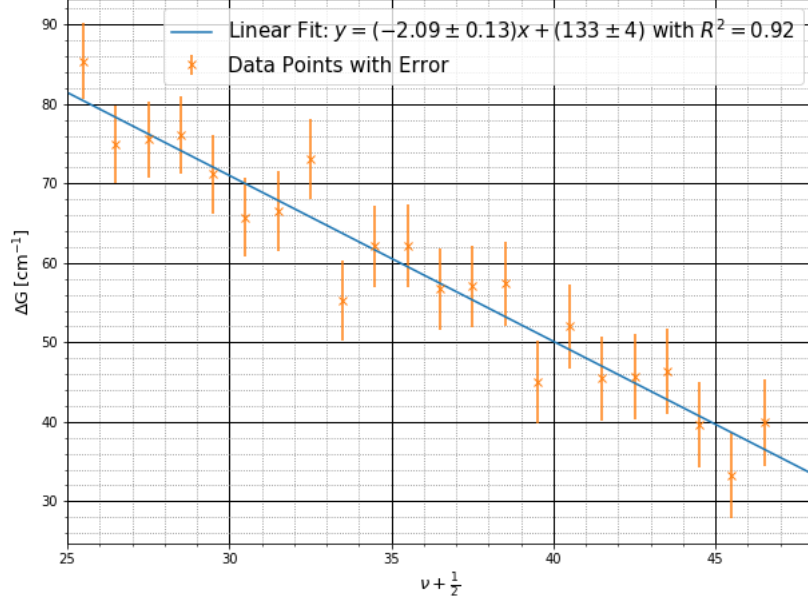


Figure 11: Birge-Sponer-Plot with Linear Fit in blue. In orange the data points of the values ΔG which can be found in table 3 with errors.

3.1.2 Dissociation Energy

We now calculate the dissociation energy D_{e1} in two different ways. First we use the equation 8 we got from the Morse Potential using both of the computed constants. The second way is using the sum in equation 11 to get the energy D_0 . By adding $G(\mu = 0)$ to this the dissociation energy D_{e2} can be calculated.

For the first method the error is calculated using the following equation:

$$\sigma_{D_e} = \sqrt{\left(\frac{\sigma_{\omega_e} \omega_e}{2\omega_e x_e}\right)^2 + \left(\frac{\sigma_{\omega_e x_e} \omega_e^2}{4(\omega_e x_e)^2}\right)^2} \quad (20)$$

With that we get for D_{e1} :

$$D_{e1} = (4300 \pm 400) \text{ cm}^{-1}$$

Now we use the second method to calculate D_0 . The error here is calculated with equation 21:

$$\sigma_{D_0} = \sqrt{\left(\sum_{\nu=0}^{\nu_{diss}} \sigma_{\Delta G(\nu+\frac{1}{2})}^2\right)} \quad (21)$$

$G(0)$ is calculated using equation 9 till the quadratic term. We get as equation to calculate $G(0)$:

$$G(0) = \frac{\omega_e}{2} - \frac{\omega_e x_e}{4}, \quad \sigma_{G(0)} = \sqrt{\left(\frac{\sigma_{\omega_e}}{2}\right)^2 + \left(\frac{\sigma_{\omega_e x_e}}{4}\right)^2} \quad (22)$$

The calculated values are:

$$D_0 = (4280 \pm 60) \text{ cm}^{-1}$$

$$G(0) = (67.1 \pm 2.4) \text{ cm}^{-1}$$

Adding these two together the error is:

$$\sigma_{D_{e1}} = \sqrt{\sigma_{G(0)}^2 + \sigma_{D_0}^2} \quad (23)$$

The value for D_{e2} is with that:

$$D_{e2} = (4340 \pm 60) \text{ cm}^{-1}$$

3.1.3 Excitation Energy T_e and Dissociation Energy E_{diss}

The energy E_{diss} is the energy between first vibration state of the electronic ground state and the dissociation state of the the exited electronic state. This energy can be found by looking at the lowest point of the spectrum where no vibration dips can be found. The estimated position can be seen in figure 12. Since this point is only an estimation we used an error of 1 nm. With that we get wavelength:

$$\lambda_{diss} = (498.22 \pm 1) \text{ nm}$$

This can be used to calculate the energy E_{diss} with equation 24.

$$E_{diss} = \frac{1}{\lambda_{diss}}, \quad \sigma_{E_{diss}} = \frac{\sigma_{\lambda_{diss}}}{\lambda_{diss}^2} \quad (24)$$

$$E_{diss} = (20070 \pm 40) \text{ cm}^{-1}$$

The connection between E_{diss} and T_e is equation 25:

$$E_{diss} \approx T_e - G'(0) + D'_e \quad (25)$$

This equation is only an approximation since $G'(0) \approx G''(0)$. We also know that

$$G'(0) + D'_e = D'_0$$

which gives the following equation to compute T_e :

$$T_e \approx E_{diss} - D'_0, \quad \sigma_{T_e} = \sqrt{\sigma_{D'_0}^2 + \sigma_{E_{diss}}^2} \quad (26)$$

$$T_e = (15790 \pm 60) \text{ cm}^{-1}$$

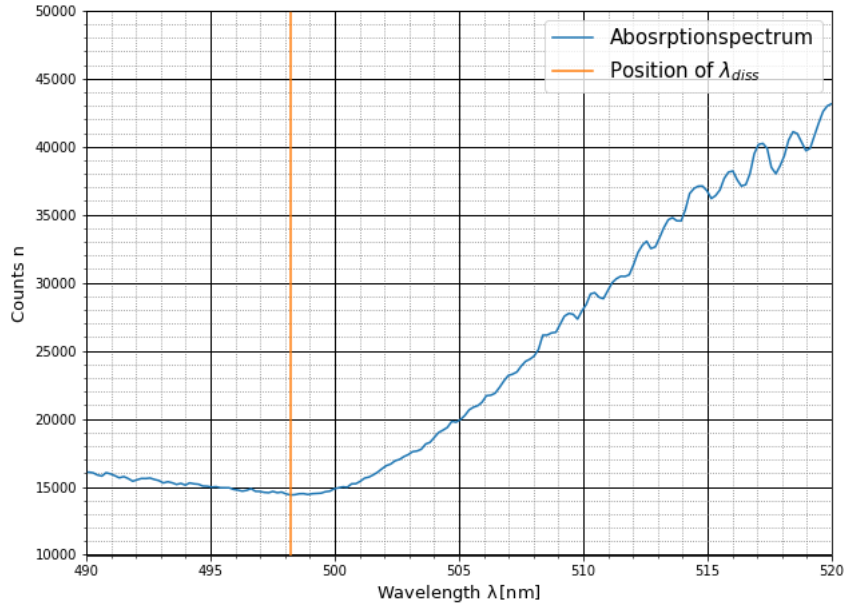


Figure 12: Segment of the absorption spectrum, which is used to calculate the to find the wavelength λ_{diss} which is marked in orange.

3.1.4 The Morse Potential

Last but not least the Morse potential shall be depicted. For this we use equation 6. The needed constants a and R_e can be calculated with:

$$a = \sqrt{\frac{\omega_e x_e 4\pi c \mu}{\hbar}} \quad (27)$$

$$R_e = \sqrt{\frac{\hbar}{4\pi c \mu B_e}} \quad (28)$$

With the constants:

$$c = 299792485 \frac{\text{m}}{\text{s}}$$

$$\mu = 1.05327 \times 10^{-25} \text{ kg}$$

$$B_e = 2.897,0.007 \text{ m}^{-1}$$

$$\hbar = 1.054571817 \times 10^{-34} \text{ J}$$

The equation for the Morse Potential is:

$$E_{Morse} = (4300 \pm 400) \text{ cm}^{-1} \left(1 - e^{-(1.98 \pm 0.06) \times 10^9 \text{ m}^{-1} (R - (3.029 \pm 0.004) \times 10^{-10} \text{ m})} \right)^2$$

This equation is plotted in figure 13.

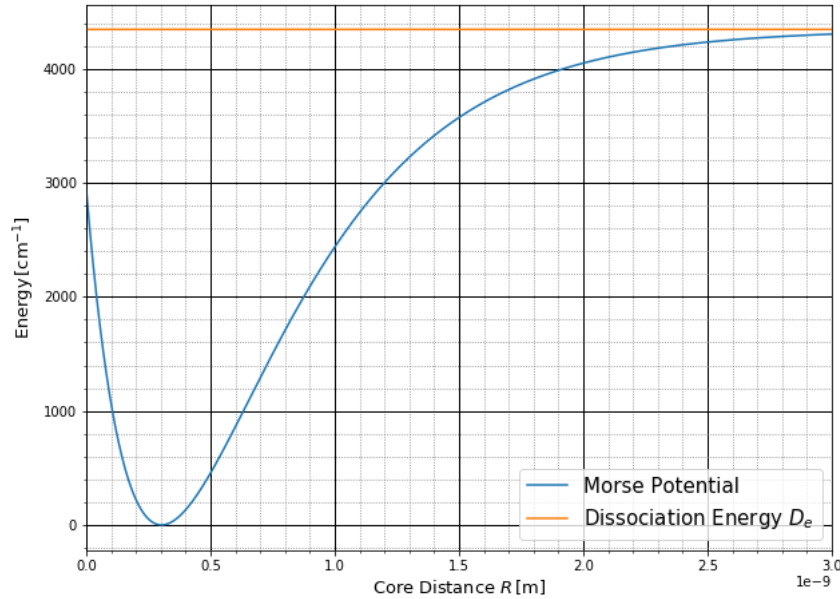


Figure 13: Morse potential with calculated values. In blue the Morse potential and in orange the dissociation energy which the Morse potential approaches for $R \rightarrow \infty$.

3.2 Emission Spectrum

3.2.1 Calibration of the Monochromator

For the calibration of the Monochromator we measured the spectrum of mercury vapour lamp. For the calibration only the data `Eichung2.csv` was used since the first one distorted during the measurement.

First of all the y values of the data were plotted against the wavelength which was calculated with the help of the starting position, end position and step width which were noted for each measurement.

The plot can be seen in figure 14. On it four different peaks are visible. Each peak was fitted with a Gaussian normal distribution of the form 29.

$$f(x) = A \frac{1}{\sqrt{2\pi\sigma^2}} \exp\left(-\frac{1}{2} \frac{(x - x_c)^2}{\sigma^2}\right) + y_c \quad (29)$$

Those fits are visible in figure 14 in red. The parameter x_c gives the position of the peak and are noted together with the literature value in table 1. This way is used for all the future data of the monochromator as well. The since the resolution wasn't high enough, the double peak couldn't be split up. That's why

| Name | Literature Value λ nm | Measured Values λ nm | $\Delta\lambda$ nm |
|---------------|-------------------------------|------------------------------|--------------------|
| h-line | 404.66 | 404.88 ± 0.05 | 0.22 ± 0.05 |
| g-line | 435.85 | 435.99 ± 0.05 | 0.14 ± 0.05 |
| e-line | 546.07 | 546.46 ± 0.05 | 0.39 ± 0.05 |
| double line 1 | 576.96 | 578.35 ± 0.04 | 1.39 ± 0.04 |
| double line 2 | 579.07 | 578.35 ± 0.04 | -0.72 ± 0.04 |

Table 1: Values of the fitted peaks as well as the literature values. There are also the differences between literature and measured value which shows a definite systematic error.

these two measurements weren't used for the calibration. By taking the difference between the literature value and the measured ones and taking the mean of them we get the value by which all our measured values will be shifted. The error is calculated using the following equation:

$$\sigma_{\Delta\lambda} = \lambda_{\text{Measured}} - \lambda_{\text{Literatur}} \quad (30)$$

With that we get a systematic shift which will be subtracted? from all further values.

$$\Delta\lambda = (0.252 \pm 0.028 \text{ nm})$$

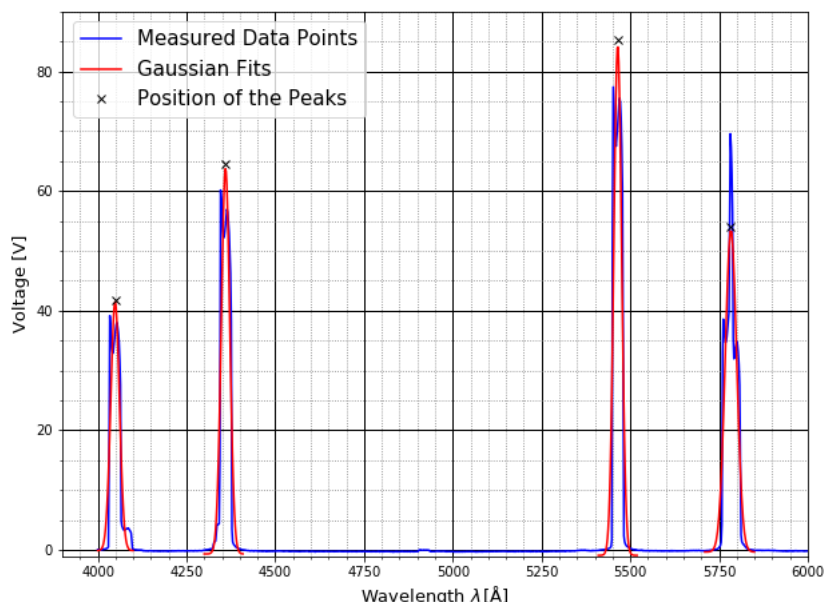


Figure 14: Peaks of the Calibration measurement with a mercury vapour lamp. In blue the measured data and in red the four Gaussian fits to the peaks.

3.2.2 Laser Peak

Next the laser peak should be depicted, for this the file `Laserpeak.csv` was used and can be found in figure 15.

Looking at data we see more like a laser plateau from 6317.5Å to 6345.5Å. Because of this the exact position couldn't be calculated but it still gives an indication in which area the peak is since the real peak will be somewhere in the area of the plateau. Since the plateau has a little drop after 6333.5 Å we can decrease the area to an interval of 6317.5Å to 6333.5Å. The Laser emits a light with a wavelength of 6330 Å which is in our designated area.

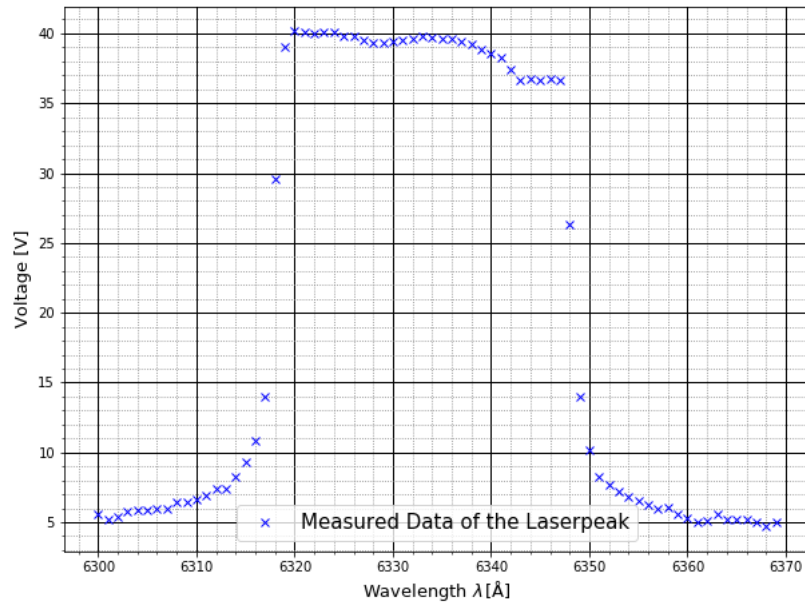


Figure 15: Measurement of the Laser Peak from 6300 Å to 6370 Å

3.2.3 I_2 Emission Spectrum

In the last part of the experiment we measured the area of 6400 Å to 8000 Å. This area was measured four times. Only the third measurement shows the later peaks clearly. The files `emissionsspektrum1.csv`, `emissionsspektrum2.csv` and `emissionsspektrum4.csv` are depicted in the appendix. Used for the analysis only the file `emissionsspektrum3.csv` was used which can be seen in figure 16. To find the

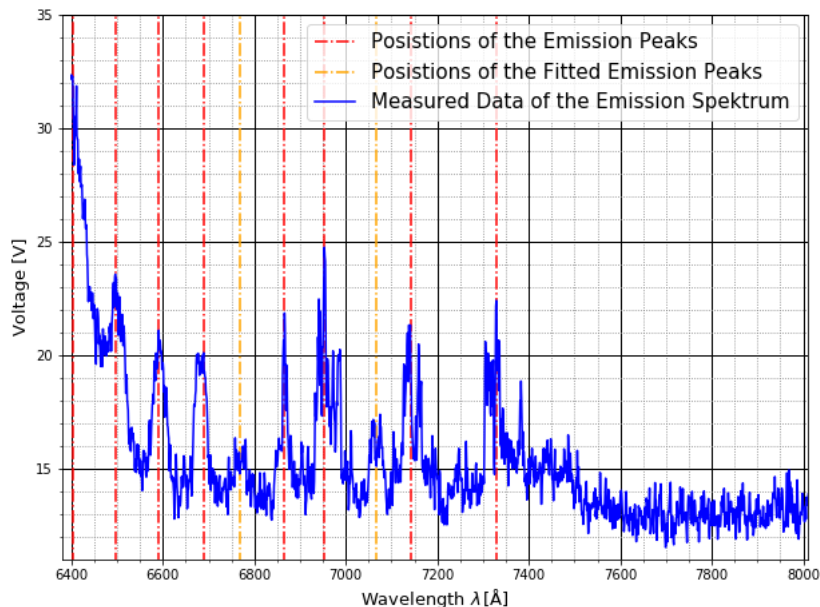


Figure 16: Emission Spectrum with the found Peaks. In orange the two smaller peaks calculated with Gaussian fits and in red the peaks found with PeakUtils.

peaks we estimated the high peaks with the help of `PeakUtils`[4] by setting a high threshold value. The peaks which were found that way are marked in the figure 16 with red lines. Since there were two smaller Peaks in between which are clearly set apart from the background those two had to be fitted. In figure 20 those two were fitted with `curve_fit` using equation 29. The position x_c of the peak is marked in orange in figure 16. As errors we estimated an error of 3 Å for the ones calculated with `PeakUtils`. For the ones fitted we used the error given by `curve_fit`.

There is also a possible peak at around 7250 Å since there is a huge gap between the peaks besides. This one is very likely hidden in the noise. The 10 found values which were measured, are in table 2.

To find out which transition we are looking at we calculate the energy of the wavelength using equation 15, which can be found in said table as well. With the help of these values the correct transitions can be found by using the table 21 which is also in the manual[3]. The comparison indicates our measured transition are $\nu' = 6 \rightarrow \nu''$ transitions by starting with $\nu'' = 4$ at the left to $\nu'' = 14$ at the right. Since there is a transition $\nu'' = 13$ we didn't find its likely that this one is the peak at 7250 Å which isn't visible. This idea is reinforced by the fact that the energy value given in table 21 for the transition $\nu'' = 13$ is fitting with the position of the missing peak.

| Transition ν'' | Wavelength $\lambda [\text{\AA}]$ | Energy $G(\nu'') [\text{cm}^{-1}]$ | Literature Value $G(\nu'') [\text{cm}^{-1}]$ | Comparison $[\sigma]$ |
|--------------------|-----------------------------------|------------------------------------|--|-----------------------|
| 4 | 6402.0 ± 3.0 | 15632 ± 7 | 15602.5068 | 3.23 |
| 5 | 6496.0 ± 3.0 | 15406 ± 7 | 15394.0768 | 0.84 |
| 6 | 6591.0 ± 3.0 | 15184 ± 7 | 15186.8608 | 1.28 |
| 7 | 6689.0 ± 3.0 | 14961 ± 7 | 14980.8588 | 3.76 |
| 8 | 6768.5 ± 1.3 | 14785.3 ± 3.1 | 14776.0708 | 1.26 |
| 9 | 6866.0 ± 3.0 | 14575 ± 6 | 14572.4968 | 0.41 |
| 10 | 6953.0 ± 3.0 | 14393 ± 6 | 14370.1368 | 2.78 |
| 11 | 7066.6 ± 0.8 | 14161.1 ± 2.0 | 14168.9908 | 7.41 |
| 12 | 7141.0 ± 3.0 | 14014 ± 6 | 13969.0588 | 6.68 |
| 13 | 7250 | 13793 | 13770.3408 | - |
| 14 | 7329.0 ± 3.0 | 13654 ± 6 | 13572.8368 | 13.59 |

Table 2: Values of the Emission Spectrum. With the likely transition and literature values. In the last column is the comparison between the calculated energy and the likely literature values. The values are compared using equation ?? and are in the units of the standard deviation.

4 Discussion of the Results

4.1 Absorption Spectrum

In the first part of the experiment we measured the absorption spectrum of iodine. First of all the constants ω_e and $\omega_e x_x$ had to be calculated by using a Birge-Sponer-Plot. The values are compared in table ?? with the literature values. The values are compared with equation ??

$$t = \frac{x_{\text{Measure}} - y_{\text{Literature}}}{\sigma_x} \quad (31)$$

Inhalt...

Tabellen

List of Tables

| | | |
|---|---|----|
| 1 | Values of the Calibration Measurement | 14 |
| 2 | Values of the Emission Spectrum | 17 |
| 3 | Values of the Transitions by Absorption | 21 |

Bilder

List of Figures

| | | |
|----|--|----|
| 1 | Franck-Condon-Principle | 2 |
| 2 | Potential Forms | 3 |
| 3 | Energy level with continuum and dissociation energy as well as D_0 that is smaller by $G(0)$. [3] | 4 |
| 4 | CCD-Spectrometer | 6 |
| 5 | Monochromator | 6 |
| 6 | Experimental Setup 1 | 7 |
| 7 | Experimental Setup 2 | 7 |
| 8 | Experimental Setup 3 | 8 |
| 9 | Complete Absorption Spectrum | 9 |
| 10 | Absorption Spectrum with Transitions | 10 |
| 11 | Birge-Sponer-Plot with Linear Fit | 11 |
| 12 | Segment of the Absorption Spectrum | 12 |
| 13 | Calculated Morse Potential | 13 |
| 14 | Calibration with Mercury Vapour Lamp | 14 |
| 15 | Laser Peak | 15 |
| 16 | Emission Spectrum with the found Peaks | 16 |
| 17 | Example of the first Emission Spectrum Measurement. | 21 |
| 18 | Example of the second Emission Spectrum Measurement. | 22 |
| 19 | Example of the fourth Emission Spectrum Measurement. | 22 |
| 20 | Fit of two Peaks in the Emission Spectrum | 23 |
| 21 | Table with Literature Values | 23 |

5 Bibliography

References

- [1] Eric Jones, Travis Oliphant, Pearu Peterson, et al. Python3 package `scipy.optimize` for curve fitting, https://docs.scipy.org/doc/scipy/reference/generated/scipy.optimize.curve_fit.html, 2001–.
- [2] Eric O. Lebigot. Python 3 package `uncertainties` for calculating with uncertainties., <https://github.com/lebigot/uncertainties/tree/master/uncertainties>, 2010–2016.
- [3] M.Meyer. Verbesserung des versuchs spektroskopie am j2-molekül des fortgeschrittenen praktikums, wissenschaftliche arbeit für das staatsexamen im fach physik, physikalisches institut albert-ludwig-universität freiburg, 2014.
- [4] Lucas Hermann Negri. Python 3 package `peakutils` for finding peaks., <https://peakutils.readthedocs.io/en/latest/>, 2014 - 2019.
- [5] Samoza. `morse-potential.png`, <https://commons.wikimedia.org/wiki/File:Morse-potential.png>, 2006.
- [6] Samoza. `franck condon diagram.svg`, https://commons.wikimedia.org/wiki/File:Franck-Condon_Diagram.svg, 2014.

6 Anhang

| ν'' | Wellenlänge λ nm | G cm $^{-1}$ | ΔG cm $^{-1}$ |
|---------|--------------------------|-------------------|-----------------------|
| 25 | 509.8 ± 0.5 | 19617 ± 4 | 40 ± 5 |
| 26 | 510.8 ± 0.5 | 19577 ± 4 | 33 ± 5 |
| 27 | 511.7 ± 0.5 | 19543 ± 4 | 40 ± 5 |
| 28 | 512.7 ± 0.5 | 19504 ± 4 | 46 ± 5 |
| 29 | 513.9 ± 0.5 | 19458 ± 4 | 46 ± 5 |
| 30 | 515.1 ± 0.5 | 19412 ± 4 | 45 ± 5 |
| 31 | 516.4 ± 0.5 | 19366 ± 4 | 52 ± 5 |
| 32 | 517.8 ± 0.5 | 19314 ± 4 | 45 ± 5 |
| 33 | 519.0 ± 0.5 | 19269 ± 4 | 57 ± 5 |
| 34 | 520.5 ± 0.5 | 19212 ± 4 | 57 ± 5 |
| 35 | 522.1 ± 0.5 | 19155 ± 4 | 57 ± 5 |
| 36 | 523.6 ± 0.5 | 19098 ± 4 | 62 ± 5 |
| 37 | 525.3 ± 0.5 | 19036 ± 4 | 62 ± 5 |
| 38 | 527.0 ± 0.5 | 18974 ± 4 | 55 ± 5 |
| 39 | 528.6 ± 0.5 | 18919 ± 4 | 73 ± 5 |
| 40 | 530.6 ± 0.5 | 18846 ± 4 | 67 ± 5 |
| 41 | 532.5 ± 0.5 | 18779.0 ± 3.5 | 66 ± 5 |
| 42 | 534.4 ± 0.5 | 18713.3 ± 3.5 | 71 ± 5 |
| 43 | 536.4 ± 0.5 | 18642.1 ± 3.5 | 76 ± 5 |
| 44 | 538.6 ± 0.5 | 18566.0 ± 3.4 | 76 ± 5 |
| 45 | 540.8 ± 0.5 | 18490.4 ± 3.4 | 75 ± 5 |
| 46 | 543.0 ± 0.5 | 18415.5 ± 3.4 | 85 ± 5 |
| 47 | 545.5 ± 0.5 | 18330.1 ± 3.4 | - |

Table 3: Wavelength and energy of the photons absorbed by the transition of $\nu' = 0 \rightarrow \nu'$. There is also the difference of energy ΔG to the next higher transition.

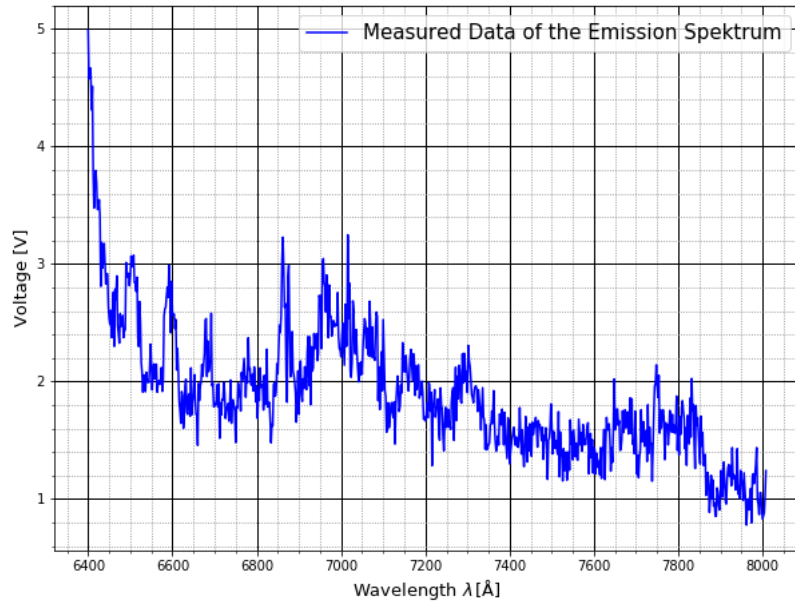


Figure 17: Example of the first Emission Spectrum Measurement.

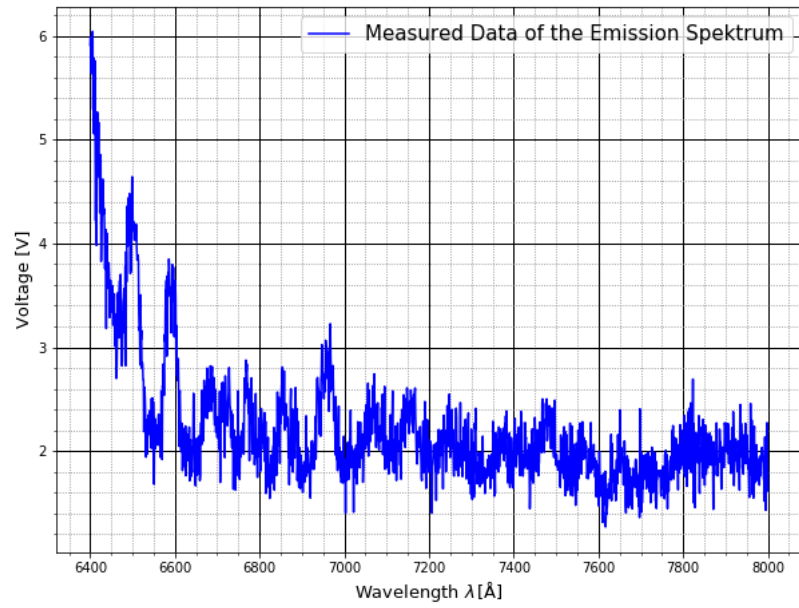


Figure 18: Example of the second Emission Spectrum Measurement.

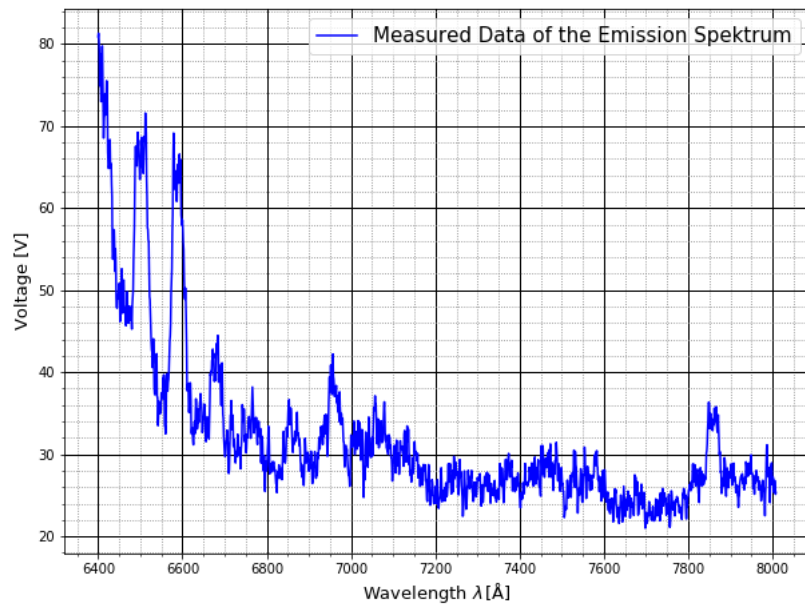


Figure 19: Example of the fourth Emission Spectrum Measurement.

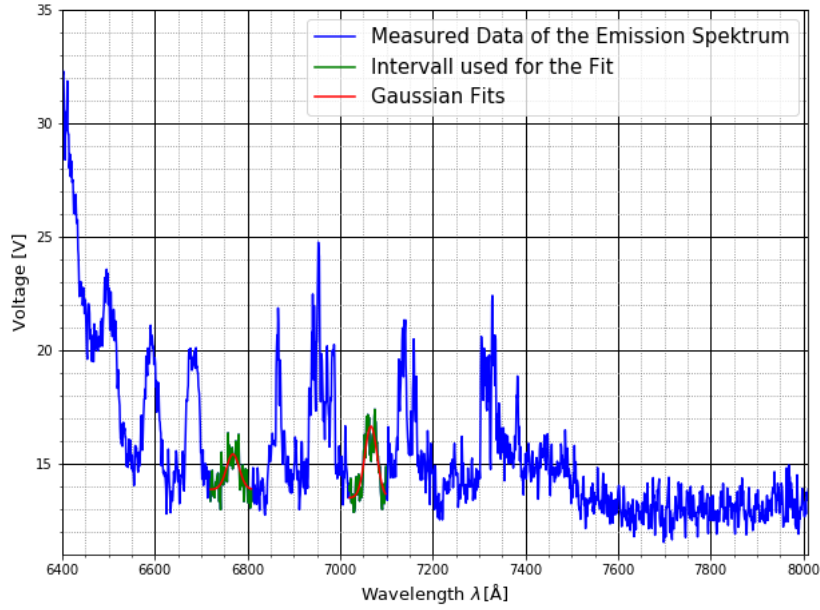


Figure 20: Fit of two Peaks in the emission spectrum. In green is the Interval of measured values used for the fit and in red the fit itself.

| ν'' | $G''(\nu'')$ | $k(\nu'=1)$ | $k(\nu'=2)$ | $k(\nu'=3)$ | $k(\nu'=4)$ | $k(\nu'=5)$ | $k(\nu'=6)$ |
|---------|--------------|-------------|-------------|-------------|-------------|-------------|-------------|
| 1 | 320,38425 | 15636,5808 | 15759,0808 | 15880,1808 | 15999,8808 | 16118,1808 | 16235,0808 |
| 2 | 532,45625 | 15424,5088 | 15547,0088 | 15668,1088 | 15787,8088 | 15906,1088 | 16023,0088 |
| 3 | 743,31425 | 15213,6508 | 15336,1508 | 15457,2508 | 15576,9508 | 15695,2508 | 15812,1508 |
| 4 | 952,95825 | 15004,0068 | 15126,5068 | 15247,6068 | 15367,3068 | 15485,6068 | 15602,5068 |
| 5 | 1161,38825 | 14795,5768 | 14918,0768 | 15039,1768 | 15158,8768 | 15277,1768 | 15394,0768 |
| 6 | 1368,60425 | 14588,3608 | 14710,8608 | 14831,9608 | 14951,6608 | 15069,9608 | 15186,8608 |
| 7 | 1574,60625 | 14382,3588 | 14504,8588 | 14625,9588 | 14745,6588 | 14863,9588 | 14980,8588 |
| 8 | 1779,39425 | 14177,5708 | 14300,0708 | 14421,1708 | 14540,8708 | 14659,1708 | 14776,0708 |
| 9 | 1982,96825 | 13973,9968 | 14096,4968 | 14217,5968 | 14337,2968 | 14455,5968 | 14572,4968 |
| 10 | 2185,32825 | 13771,6368 | 13894,1368 | 14015,2368 | 14134,9368 | 14253,2368 | 14370,1368 |
| 11 | 2386,47425 | 13570,4908 | 13692,9908 | 13814,0908 | 13933,7908 | 14052,0908 | 14168,9908 |
| 12 | 2586,40625 | 13370,5588 | 13493,0588 | 13614,1588 | 13733,8588 | 13852,1588 | 13969,0588 |
| 13 | 2785,12425 | 13171,8408 | 13294,3408 | 13415,4408 | 13535,1408 | 13653,4408 | 13770,3408 |
| 14 | 2982,62825 | 12974,3368 | 13096,8368 | 13217,9368 | 13337,6368 | 13455,9368 | 13572,8368 |
| 15 | 3178,91825 | 12778,0468 | 12900,5468 | 13021,6468 | 13141,3468 | 13259,6468 | 13376,5468 |
| 16 | 3373,99425 | 12582,9708 | 12705,4708 | 12826,5708 | 12946,2708 | 13064,5708 | 13181,4708 |
| 17 | 3567,85625 | 12389,1088 | 12511,6088 | 12632,7088 | 12752,4088 | 12870,7088 | 12987,6088 |
| 18 | 3760,50425 | 12196,4608 | 12318,9608 | 12440,0608 | 12559,7608 | 12678,0608 | 12794,9608 |
| 19 | 3951,93825 | 12005,0268 | 12127,5268 | 12248,6268 | 12368,3268 | 12486,6268 | 12603,5268 |
| 20 | 4142,15825 | 11814,8068 | 11937,3068 | 12058,4068 | 12178,1068 | 12296,4068 | 12413,3068 |
| 21 | 4331,16425 | 11625,8008 | 11748,3008 | 11869,4008 | 11989,1008 | 12107,4008 | 12224,3008 |
| 22 | 4518,95625 | 11438,0088 | 11560,5088 | 11681,6088 | 11801,3088 | 11919,6088 | 12036,5088 |
| 23 | 4705,53425 | 11251,4308 | 11373,9308 | 11495,0308 | 11614,7308 | 11733,0308 | 11849,9308 |
| 24 | 4890,89825 | 11066,0668 | 11188,5668 | 11309,6668 | 11429,3668 | 11547,6668 | 11664,5668 |
| 25 | 5075,04825 | 10881,9168 | 11004,4168 | 11125,5168 | 11245,2168 | 11363,5168 | 11480,4168 |
| 26 | 5257,98425 | 10698,9808 | 10821,4808 | 10942,5808 | 11062,2808 | 11180,5808 | 11297,4808 |
| 27 | 5439,70625 | 10517,2588 | 10639,7588 | 10760,8588 | 10880,5588 | 10998,8588 | 11115,7588 |

Figure 21: Figure of the table with literature values used for the analysis of the emission spectrum.[3]